

Original scientific paper

Received:25.7.2019

Accepted:29.11.2019

UDK: 674.06:674.028.9]:[519.876.2:539.4

**NUMERICAL MODELING OF WOOD-ADHESIVE BOND-LINE IN MODE II
FOR SPRUCE WOOD GLUED BY VARIOUS ADHESIVES**

Václav Sebera^{1,3*}, Jaka Gašper Pe nik^{1,3}, Boris Azinovi ², Miha Kramar²

¹ *InnoRenew CoE, Izola, Slovenia,*

² *Slovenian Building and Civil Engineering Institute, Ljubljana, Slovenia,*

³ *University of Primorska, Koper, Slovenia*

vaclav.sebera@innorenew.eu

ABSTRACT

Bond-line creates an interface between two glued surfaces and, therefore, it brings additional complexity into the mechanical behavior of glued components, especially around the bond-line region, because an adhesive has a very different response to a mechanical stress than wood. From this perspective, the bond-line influences the total mechanical response of glued components by both its cohesive and adhesive behavior at wood-adhesive boundary. For timber constructions, there are many various adhesives one can use and each of them has a different mechanical characteristics, advantages and disadvantages.

The goal of this work was to create a numerical finite element models applicable for analysis of fracture problems in mode II. The models were developed for the adhesives that are often applied in timber constructions and wooden materials. The FE models include 2D geometry of the bond line and cohesive law fitted on the outputs of the experimental measurement. The experimental data for the developing numerical models were obtained using 3point end-notched flexure (3ENF) tests with the compliance-based beam method (CBBM) coupled with the digital image correlation to be able to obtain displacement slip needed for the development of the FE models. Furthermore, within the FE analysis, wood was modeled as orthotropic material including both elastic and plastic regions of deformation. The FE models were developed in Ansys computational system. The specific objectives of the work were as follows: 1) to create cohesive zone models based on experimental data; 2) to develop parametric 2D and 3D model of the bond-line reflecting experimental data; 3) to analyze the influence of friction coefficient on resulting force-displacement outputs; and 4) to analyze plastic imprint into the specimens for Norway spruce and the influence of the fiber angle inclination.

Implementation of cohesive law models of wood-adhesive system into the FE analysis was successful. The FE analysis provided the force-deflection response that was validated by the experiment work. The FE model showed that influence of friction on simulated force may be up to 5% of the maximal force, which is not a negligible effect. The imprint of the load head into specimen is substantial if span-to-height ratio is below 17. The influence of the fiber angle with respect to a longitudinal axis is rather high, i.e. angle of 14° means 30% reduction of maximal force.

Key words: mode II, spruce wood, finite element analysis, crack propagation, adhesive bond

1. INTRODUCTION

Wood is one of a few structural renewable materials with high strength-to-density ratio that can be widely used. The use of wood in constructions is limited by the size of the input source material. Therefore, there is always a need to use bonding techniques such as gluing, to fully utilize the material potential. The potential can be easily seen in wood-based composites (WBCs) such as Glulam, Cross-

Laminated Timber (CLT), plywood and many others. Using a full potential of the WBC's can be, and actually it already is, intensified by computational techniques that can be used to various purposes – structural analysis, optimizations etc. Since WBCs often contain bondline, numerical modeling of the bond line is also of great interest within the research. The bondline is an important feature in numerical models of WBCs. The bondline is often neglected and wooden parts are assumed to be perfectly and elastically connected, so there is no need to define material model of adhesive. Another approach is to define the bondline as a separate material using cohesive zone model (CZM), which allows to model fracture phenomena – development and propagation of crack. With respect to this work and WBCs embedded in constructions, one of the important modes of crack propagation is in mode II – shear mode developing during bending or horizontal forces (Yoshihara, 2001).

Experimentally, fracture properties of wood have been measured using ENF in bending test for a long time. Yoshihara and Ohta (2000) showed that fracture properties of wood are dependent on a ratio of initial crack length and half span which has to be reflected in an experiment design. De Moura et al. (2006) employed so called equivalent crack approach and incorporated it into the compliance-based beam method (CBBM). This combination showed to be advantageous because it did not require tracking of crack propagation which was, to a convenience, derived directly from the current compliance. The equivalent crack length method applied on a pine wood was examined by Silva et al. (2006). These authors also developed the finite element (FE) model of a crack propagation of wood in mode II that was successfully verified using equivalent crack length approach. Silva et al. (2007) successfully tested procedure of equivalent crack experimentally and numerically on end load split (ELS) scheme when examining fracture properties of pine wood in mode II. Because of its relative ease, the ENF with equivalent crack approach is well suited for wood bonds (Xavier et al., 2011) and for determination of cohesive zone models of material itself or adhesive bonds that may be used in numerical simulations (Silva et al., 2014). Meite et al. (2013) employed optimization technique within a combination of finite element simulation and DIC analysis to characterize fracture behavior of Douglas fir wood (*Pseudotsuga menziesii* L.) in mixed mode. Both tools conveniently provided data that enabled separation of mode I and mode II without taking into account local elastic mechanical properties.

The goal of the paper is to develop a numerical model of crack propagation in mode II with use of elastic and plastic material models. The work should contribute to the bondline FE modeling used in WBCs analyses.

2. MATERIAL AND METHODS

Within the work, we developed two kinds of the FE model of 3point end-notched flexure (3ENF) test. The first one was two-dimensional (2D) model and the second was three-dimensional (3D). The 2D FE model was developed to investigate an influence of friction coefficient on force-deflection response. The 3D model was developed to investigate fiber angle declination and adhesive bond on force-deflection response, as well as for stress distribution, imprint and strain energy in total model and under the loading head and above supports.

2D FE model

For a development of the 2D FE model (Figure 1), we used Ansys v 19.2 (Ansys Inc., USA). The FE model employed 4 different types of finite elements: 1) Plane183 for modeling the main body of the sample. This FE is quadratic element consisting of 8 nodes, each node has three degrees of freedom (displacements in X, Y and Z directions) that enables elastic orthotropic material properties; 2) contact elements Targe169 and Conta172 for modeling contact phenomena between the sample and supports and loading head. The supports and loading grip were modeled as perfectly rigid because they are made of steel and, hence, the contact pairs were defined as rigid-flexible; 3) Inter203 that is quadratic 6node element. This element was employed to model cohesive zone in the middle of the sample – in a position of highest shear stress – neutral axis. All the 2D analyses assumed plane stress with a real thickness (defined as real parameter).

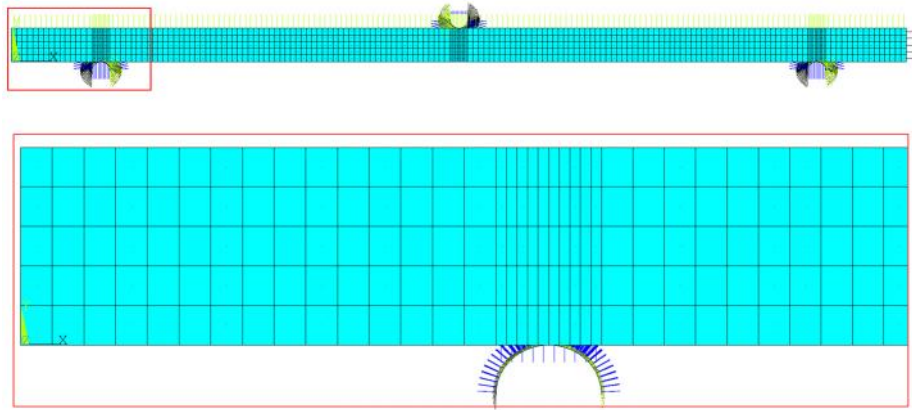


Figure 1. Finite element mesh of 2D model , top – whole FE model of the analysis; bottom – detail on support and FE mesh including contact elements

Boundary conditions of the 2D model reflected 3point end-notched flexure (3ENF) test setup (Figure 2) and consisted of: 1) constraining all DOFs of the supports; 2) prescribing the displacement of the loading head to 10 mm aiming downwards. The displacement of the loading head was controlled via so called “pilot node” that was also used to investigate reaction forces during the analysis. All the defined contacts were set to “close gap”, so contact began immediately at the first step of the analysis.

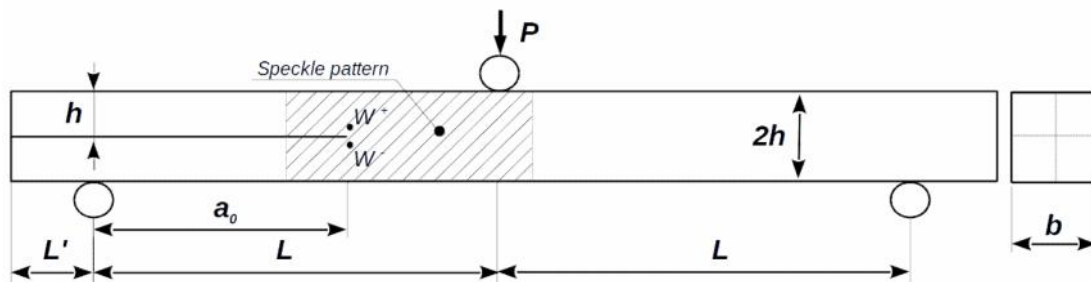


Figure 2. Geometry of sample and sketch of the 3ENF test

The analysis was solved with a nonlinear option “large deformation”. Material model used for spruce wood was elastic orthotropic taken from Milch J. et al. (2016), it is as follows: $E_L = 17\ 850$ MPa, $E_T = 289$ MPa, $E_R = 352$ MPa, $G_{LR} = 573$ MPa, $G_{LT} = 474$ MPa, $G_{RT} = 53$ MPa, $\nu_{LR} = 0.023$, $\nu_{LT} = 0.014$, $\nu_{RT} = 0.557$, where E_i is normal modulus, G_{ij} is shear modulus and ν_{ij} is Poisson’s ratio. For the cohesive zone, we employed bilinear model of traction-separation law with maximal shear stress = 5 MPa and opening 0.05 mm at this level of shear stress.

3D FE model

3D FE model was developed also in Ansys v 19.2 (Figure 3). Due to different dimensionality, we used the following types of finite elements: 1) Solid95 for modeling the main body of the sample. This FE is a quadratic element consisting of 20 nodes, each node has three degrees of freedom (displacements in X, Y and Z directions) and it enables elastic-plastic orthotropic material properties. The FE plasticity follows the generalized Hill potential theory; 2) 3D contact elements Targe170 and Conta174 for modeling contact phenomena between the sample and supports and loading head, both are quadratic elements. The supports and loading grip were modeled as perfectly rigid similarly to 2D FE model; 3) Inter205 that is 3D quadratic 8-node element.

The analysis was solved with a nonlinear option “large deformation”. Material model used for spruce wood was orthotropic elasto-plastic taken from Milch J. et al. (2016). The elastic part is the same as for 2D model, the plasticity was defined as follows: 1) three yield stresses in normal directions: $\sigma_L = 49$ MPa, $\sigma_R = 6.4$ MPa, $\sigma_T = 7.1$ MPa; 2) three tangent moduli in normal directions:

$E_{L,tan} = 140$ MPa, $E_{R,tan} = 1.8$ MPa, $E_{T,tan} = 2.3$ MPa; 3) three shear yield stresses: $\sigma_{LR} = 6.7$ MPa, $\sigma_{RT} = 6.7$ MPa and $\sigma_{LT} = 3.1$ MPa.; 4) three shear tangent moduli: $E_{LR,tan} = 5.73$ MPa, $E_{LT,tan} = 4.74$ MPa, $E_{RT,tan} = 0.53$ MPa. The elasto-plasticity was simplified in a way that we assumed the same properties in tension and compression mode. For the cohesive zone, we employed bilinear model of traction-separation law with maximal shear stress $\tau = 5$ MPa and opening 0.05 mm at this level of shear stress.

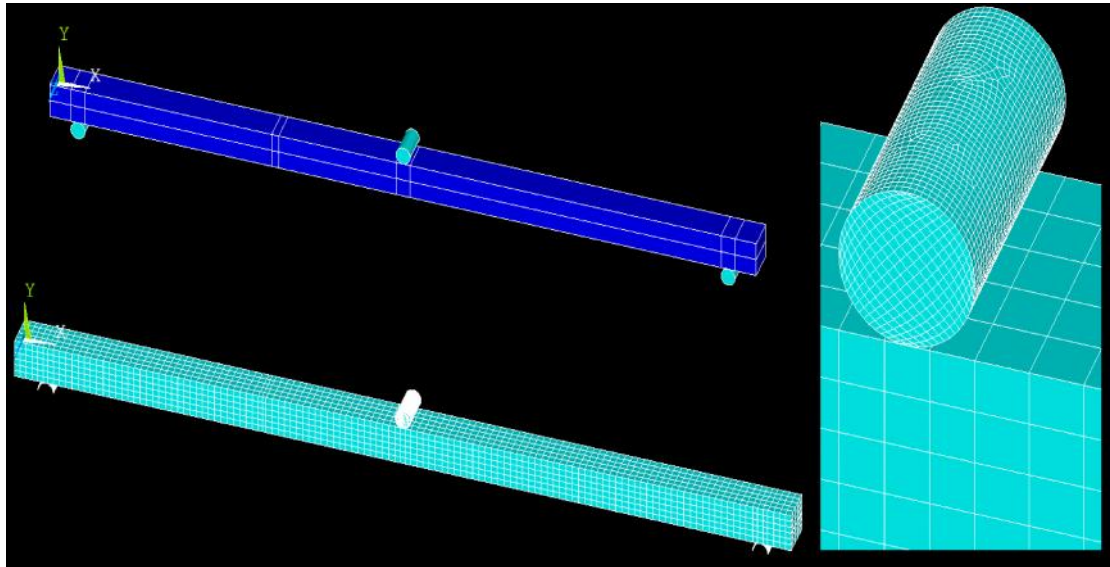


Figure 3. Finite element mesh of 3D model , top – whole geometrical model, bottom – whole FE model, right – detail of FE mesh at the loading grips

3. RESULTS AND DISCUSSION

2D FE model

The purpose of the 2D FE model was to analyze the impact of friction coefficient on resulting force-deflection diagrams. The result of this analysis is shown in Figure 4 which reveals that the coefficient of friction (f) that is applied inside the introduced crack increases both stiffness and maximal force.

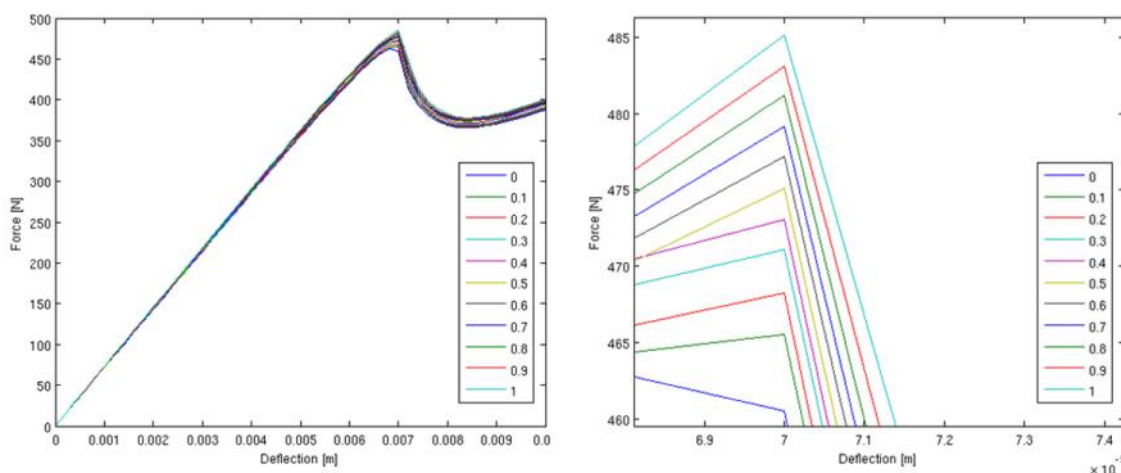


Figure 4. Left – influence of friction coefficient on force-deflection response in 2D FE model, right – detail of the maximal values for

The effect of f on the maximal force (F_{max}) shows there is 5.2% difference when comparing scenarios with minimal and maximal f (i.e. $f = 0$ and $f = 1$). Despite the fact that it seems that f has a

low impact on F_{max} , we have to recall that the 3ENF is used for measuring critical energy strain release rate ($G_{II,c}$) that is taken from the maximal force achieved. Therefore, even such a slight difference should not be neglected. From this point of view, it is fully justified to insert a Teflon paper into the introduced crack to reduce friction between the two parts during experimental measurement. The influence of the f on stiffness (S) is lower and it is about 3%.

3D FE model

Influence of the span/height ratio

The first analysis focused on the influence of specimen slenderness – span to height ratio (S/h). The result of this analysis for various S/h ratios in terms of the total strain energy is depicted in Figure 5. In Figure 5 on the left, we can see the strain energies for the regions of the specimen above supports (1cm to each side from the center of the contact). We see that if the analysis is made around the supports, there are not many differences for S/h ratios above 15. It is also possible to see that there is not much differences in a summation of plastic energies for regions of supports.

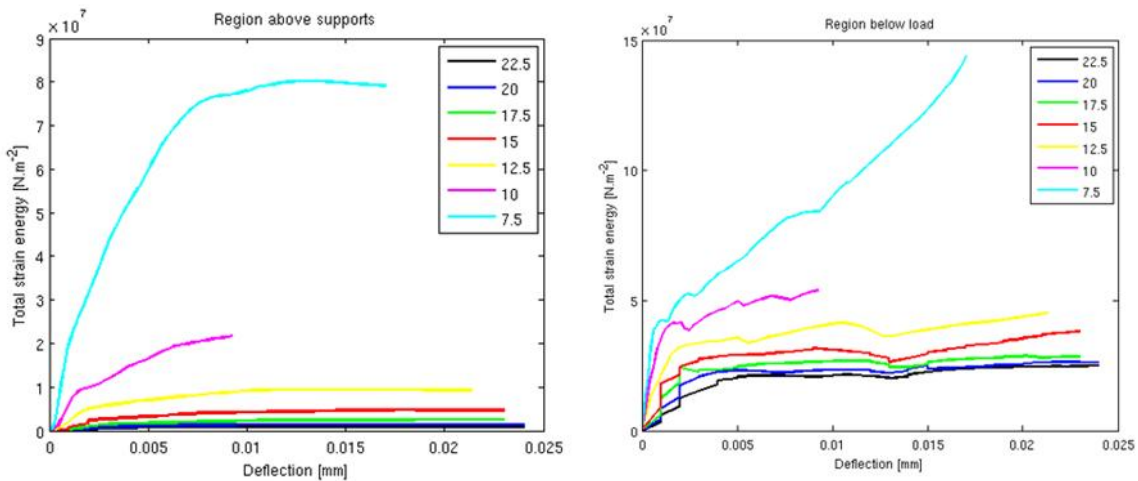


Figure 5. Influence of span/height ratio on a total strain energy: left – regions above supports, right – region below the load head

Contrary to this, the situation is much clearer with the region below the load head (Figure 5 right). We clearly see that S/h ratio above or equal to 17.5 means almost the same strain energy for plastic region of deformation. This means that the plastic imprint into the material is minimized and plastic deformation is done due to the bending itself, not due to the contact with load head. This finding agrees with Yoshihara (2001) who stated that for 3ENF test we shall use the S/h ratio above 17 to successfully obtain fracture properties such as $G_{II,c}$.

The distribution of plastic strain energy for the S/h = 10 is depicted in Figure 6. We can observe that on the tension side of the specimen, plastic energy is logically distributed and reflects the material deformation due to bending. On the contrary, the significant imprint due to a contact with a load head (i.e. region below load head) leads to a different distribution and increased plastic strain energy.

For a clarity, a stress distribution in the sample with S/h= 10 for the maximal deflection is depicted in Figure 7. Figure 7 left shows the stress parallel to the fiber, and we can clearly see the significant imprint into the material, and that stress distribution at the compression side is strongly influenced by the load head. This influence is visible even more on a distribution of stress perpendicular to fiber (parallel to force) which is depicted in Figure 7 right.

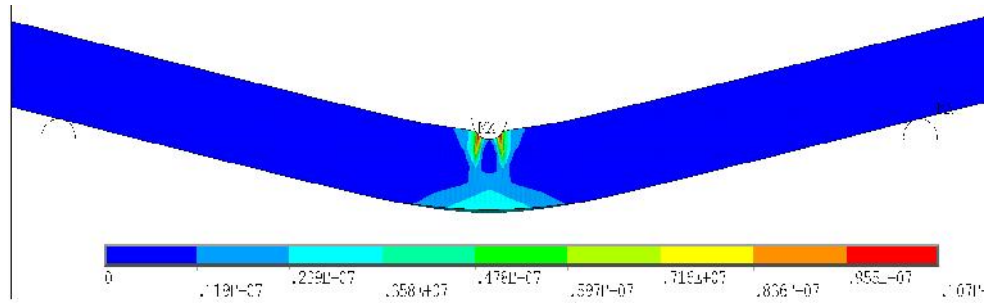


Figure 6. Plastic strain energy distribution for scenario $S/h = 10$

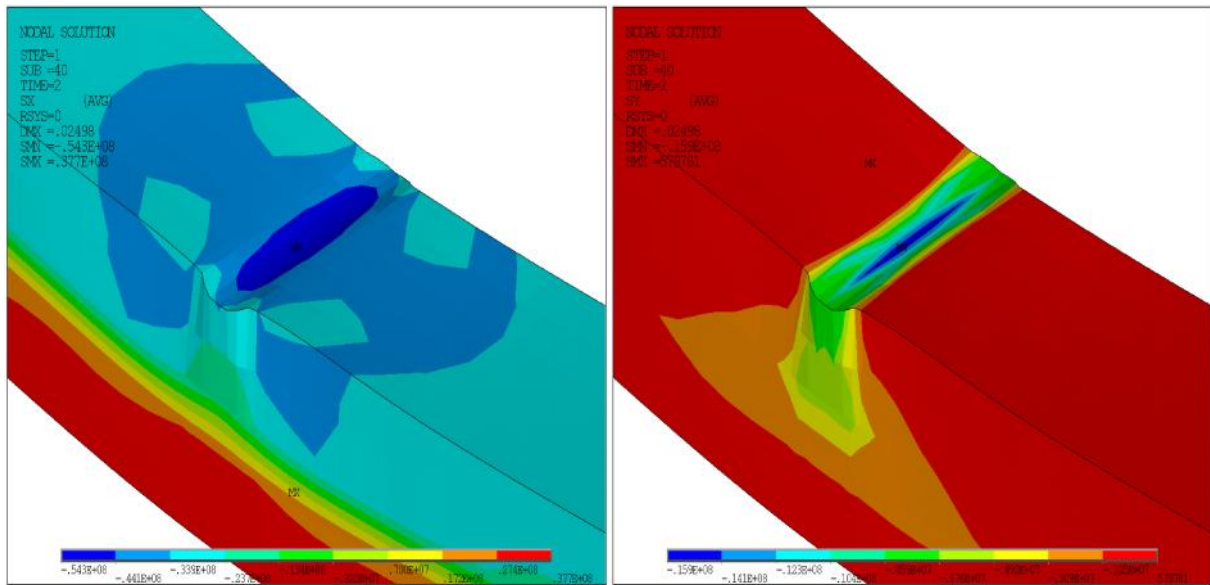


Figure 7. Stress distribution for scenario $S/h = 10$ at maximal deflection, left – stress in X axis direction (fiber direction), right – stress in Y axis direction (perpendicular to fiber and parallel to applied force)

Influence of the grain angle

The first analysis examined an influence of the grain angle inclination with respect to longitudinal axis of the sample. The angle was varied from 0 to 14 degrees with a step of 2° which resulted in 7 FE simulations. The results of these simulations are depicted in Figure 8 left. We clearly see that the angle inclination substantially influences both stiffness and maximal force. The inclination of 14° resulted in maximal force equal to approx. 70% of force with zero inclination. The stiffness of the scenario with the inclination of 14° was 42% of stiffness with zero inclination.

The second analysis examined an influence of the grain angle inclination with respect to cross-section plane (radial-tangential plane) of the specimen. The angle was varied from 0 to 90 degrees with a step of 10° which resulted in 9 FE simulations. The angle 0° means that the bending force acted in radial direction, and the angle 90° represents a pure tangential loading. The results of these simulations are shown in Figure 8 right. We can see that the radial-dominated scenarios have slightly lower maximal forces (2% lower) than tangential-dominated scenarios and, moreover, they exhibit rather more brittle behavior than tangential-dominated scenarios – first 5 scenarios show a certain peak where failure of adhesive bond occurs, meanwhile the second 5 scenarios have rather wider plastic regions. The different behavior in radial and tangential directions reflects the difference in material properties in both directions.

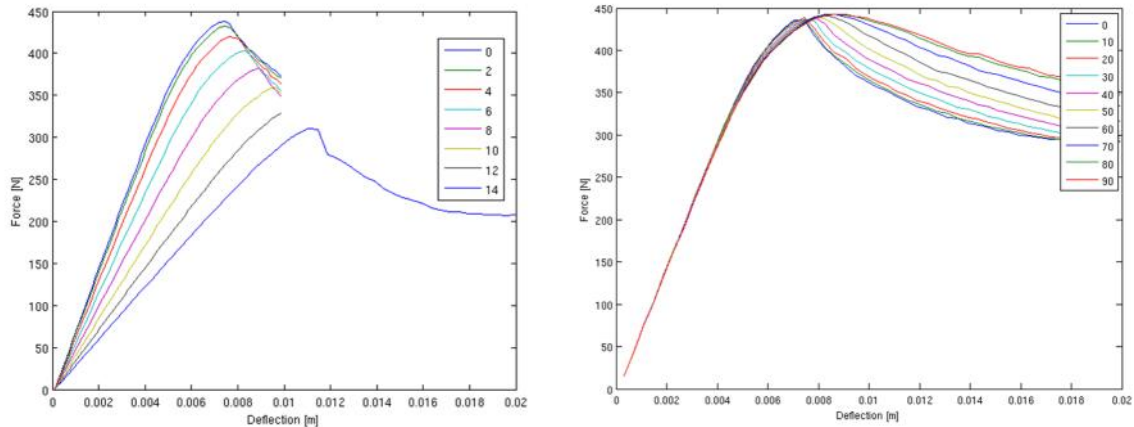


Figure 8. Stress distribution for scenario $S/h = 10$ at maximal deflection, left – stress in X axis direction (fiber direction), right – stress in Y axis direction (perpendicular to fiber and parallel to applied force)

4. CONCLUSIONS

Two parametric FE models that included cohesive zone model and orthotropic elasto-plastic material were created using APDL in Ansys FE package. The 2D FE models showed the influence of the friction coefficient on the outputs of 3ENF test. These results justified using Teflon paper to be inserted in the crack during the measurement to obtain more precise values of strain energy release rate (G_{II}). The 3D FE model showed that it is necessary to have span-to-height ratio over 17 to avoid plastic deformation below the load head which will consequently result in inducing a deformation of the sample only by bending. The grain angle inclination, either with respect to longitudinal or perpendicular specimen axes, influences both stiffness and maximal forces (F_{max}). The longitudinal grain angle of 14° may cause 30% reduction in F_{max} and 42% in stiffness.

Acknowledgement

European Commission for funding the InnoRenew CoE project under the Horizon2020 Widespread-Teaming program [Grant Agreement #739574] and the Republic of Slovenia for providing support from the European Regional Development Funds.

REFERENCES

- [1] de Moura, M. F. S. F., Silva, M. A. L., de Morais, A. B., & Morais, J. J. L. (2006). Equivalent crack based mode II fracture characterization of wood. *Engineering Fracture Mechanics*, 73(8), 978–993.
- [2] Méité, M., F. Dubois, O. Pop, and J. Absi. “Mixed Mode Fracture Properties Characterization for Wood by Digital Images Correlation and Finite Element Method Coupling.” *Engineering Fracture Mechanics* 105 (June 2013): 86–100.
- [3] J. Milch, J. Tippner, V. Sebera, M. Brabec: Determination of the elasto-plastic material characteristics of Norway spruce and European beech wood by experimental and numerical analyses. *Holzforschung* 70 (2016), 1081-1092.
- [4] Silva, M. A. L., de Moura, M. F. S. F., & Morais, J. J. L. (2006). Numerical analysis of the ENF test for mode II wood fracture. *Composites Part A: Applied Science and Manufacturing*, 37(9), 1334–1344.
- [5] Silva, M. A. L., Morais, J. J. L., de Moura, M. F. S. F., & Lousada, J. L. (2007). Mode II wood fracture characterization using the ELS test. *Engineering Fracture Mechanics*, 74(14), 2133–2147.

- [6] Silva, F. G. A., Morais, J. J. L., Dourado, N., Xavier, J., Pereira, F. A. M., & De Moura, M. F. S. F. (2014). Determination of cohesive laws in wood bonded joints under mode II loading using the ENF test. *International Journal of Adhesion and Adhesives*, 51, 54–61.
- [7] Xavier, J., Morais, J., Dourado, N., & De Moura, M. F. S. F. (2011). Measurement of mode I and mode II fracture properties of wood-bonded joints. *Journal of Adhesion Science and Technology*, 25(20), 2881–2895.
- [8] Yoshihara, H. (2001). Influence of span/depth ratio on the measurement of mode II fracture toughness of wood by end-notched flexure test, 8–12.
- [9] Yoshihara, H., & Ohta, M. (2000). Measurement of mode II fracture toughness of wood by the end-notched flexure test. *Journal of Wood Science*, 46, 273–278.

Václav Sebera, Ph.D.^{1,3},
M.Sc. Jaka Gašper Pe nik^{1,3}
Boris Azinovi , Ph.D.²
Miha Kramar, Ph.D.²

¹ *InnoRenew CoE, Livade 6, Izola, Slovenia,*

² *Slovenian Building and Civil Engineering Institute, Dimi eva ulica 12, Ljubljana, Slovenia*

³ *University of Primorska, FAMNIT, Glagoljaška ulica 8, Koper, Slovenia*

e-mail: vaclav.sebera@innorenew.eu